

Effects of the impurity potential on the band structure of doped trans-polyacetylene

This article has been downloaded from IOPscience. Please scroll down to see the full text article.

1993 J. Phys.: Condens. Matter 5 3351

(<http://iopscience.iop.org/0953-8984/5/20/008>)

View [the table of contents for this issue](#), or go to the [journal homepage](#) for more

Download details:

IP Address: 171.66.16.159

The article was downloaded on 12/05/2010 at 14:03

Please note that [terms and conditions apply](#).

Effects of the impurity potential on the band structure of doped *trans*-polyacetylene

J M Dong†, R Y Jia‡ and D Y Xing†§

† Department of Physics and National Laboratory of Solid State Microstructures, Nanjing University, Nanjing 210008, People's Republic of China

‡ Department of Physics, Beijing Normal University, Beijing 100875, People's Republic of China

§ Centre of Theoretical Physics, China Centre of Advanced Science and Technology (World Laboratory), PO Box 8730, Beijing 100080, People's Republic of China

Received 11 June 1992, in final form 25 November 1992

Abstract. In order to understand the drastic effect of impurity doping on the transport properties of polyacetylene, we investigate in detail how the impurity ion potential alone affects the band structure of electrons and the order parameter in doped polyacetylene by a self-consistent numerical calculation based upon the Su–Schrieffer–Heeger Hamiltonian plus the impurity potential. Our results show that the potential has only a small effect on gap closure, which is mainly determined by the larger overlap between the electronic wavefunctions in the nearest soliton states. We also find that the order parameter does not go to zero in the heavily doped region where there is no gap, and it is almost unaffected by the impurity potential.

1. Introduction

Doping polyacetylene with impurities has drastic effects on its properties. When the doping concentration y is very low ($y < 0.001$), it is an insulator or semiconductor having an energy gap of about 1.8 eV. On further doping, its conductivity σ can rise very rapidly up to $y \simeq 0.01$. In the regime $0.01 < y < 0.06$, its conductivity σ still increases rapidly but, more importantly, its Pauli susceptibility χ_P has a very small value [1]. Finally, when $y > 0.06$, it becomes a metal with a high σ and a traditional metallic value of χ_P . A recently developed fine technique can synthesize polyacetylene having more perfect chains with large average conjugation lengths, and so the electrical conductivity in the heavily doped sample can become greater than $1.5 \times 10^5 \Omega^{-1} \text{ cm}^{-1}$ [2]. However, it is never an ordinary metal because the dependence of conductivity on temperature shows a non-metallic behaviour, i.e. decreasing with decreasing temperature.

It seems that there is no unified theoretical model which can explain well the impurity effects in polyacetylene for all doping regimes. The Su–Schrieffer–Heeger (SSH) model [3] gives a physical picture of the new type of soliton excitation in pure and doped polyacetylene. So, the electric, magnetic and optical properties can be explained well on the basis of the soliton picture for the low-doping regime. For the intermediate- and heavy-doping regimes there have been various theoretical models discussing the impurity effects on the physical properties of doped polyacetylene. Among them are the variable-range hopping mechanism [4], soliton transport [5], polaron lattice [6], thermal-fluctuation-induced tunnelling between metallic particles [7], destruction of the gap at high impurity concentration by the dopant

random distribution [8], and finally the gap closure model [9]. All these mainly concern electronic transport.

Although in real doped materials a random distribution of impurities may be possible, the conduction mechanism based upon only disorder has a serious drawback because well ordered dopant distribution regions are proved to exist by x-rays and neutron scattering, at least for Na-doped $(\text{CH})_x$ [10]. Also, infrared absorption experiments [11] established that up to a doping level of about 18%, soliton levels still exist. Conwell *et al* [9] analysed carefully many different experiments and concluded that the soliton lattice exists even for the heavy-doping regime, and the carriers added (electrons or holes) because of doping go into the soliton lattice [9, 12]. We know that doping usually has two main effects on material. One is simply to increase the number of charge carriers in polyacetylene (electrons or holes, depending on whether the dopants are donors or acceptors; hereafter, we are considering only the donor case). This effect may be less important, especially in the heavy-doping regime. Another is that the dopants become charged ions and have a Coulomb interaction with all charge carriers on the polyacetylene chains. This impurity potential can pin the soliton lattice and has rather a large effect on the band structure of electrons in *trans*-polyacetylene. This is because the impurity ions lie between chains and its distance to the nearest-neighbour chain is rather short, only about 2–2.5 Å; moreover the transverse screening is much weaker. The usual theories do not include the effects of the impurity ion potential and so can only be applied to the pure or low-doping cases. Bryant and Glick [13] calculated the effect of a single impurity ion on the distribution of energy levels in the conduction and valence bands and found that the effect is rather strong. Without the ion potential, theoretical calculation found that above 6% doping the energy gap still exists. Even when the ion potential effect on only the nearest-neighbour C atom is included, the calculation found that the gap still did not disappear [14]. Conwell *et al* [9] calculated the band structure for a chain of doped *trans*-polyacetylene including the Coulomb potential caused by both dopant ions and charged solitons surrounding the chain. They found that the energy gap does not disappear completely for the heavy-doping regime, but that a small gap, about 0.1 eV, remains at the Fermi energy. Because the gap is small, the behaviour at room temperature could be metallic but, at low temperatures, it should be semiconducting.

2. Model

From the description given above we see that in order to clarify why doping has so drastic an effect on the transport properties of polyacetylene, it is important to investigate in detail how the impurity ion potential alone affects the band structure of electrons and the order parameter of doped polyacetylene. This paper will do that by self-consistent numerical calculation of the SSH Hamiltonian plus the impurity potential. The Hamiltonian that we have used in calculation is written as

$$H = - \sum_{n\sigma} [t_0 - \alpha(u_{n+1} - u_n)](c_{n+1,\sigma}^+ c_{n\sigma} + \text{HC}) + \frac{K}{2} \sum_n (u_{n+1} - u_n)^2 + \sum_{n\sigma} V_n c_{n\sigma}^+ c_{n\sigma} \quad (1)$$

where t_0 is the transfer integral of electrons in the undimerized state, u_n is the displacement of the n th lattice site, α is the electron-phonon coupling constant, K is the elastic constant, and $c_{n\sigma}^+$ and $c_{n\sigma}$ are the creation and annihilation operators of a π -electron with spin σ at the n th site. V_n is the Coulomb potential due to all impurity ions at the n th site:

$$V_n = - \sum_i \frac{ee_i}{\epsilon[(n - n_i)^2 a^2 + r_i^2]^{1/2}} \quad (2)$$

where $-e$ is the electron charge, e_i the i th ion charge, n_i the coordinate of the i th ion along the chain, a the lattice constant, r_i the perpendicular distance of the i th ion from the chain and ϵ the dielectric constant. Here, for simplicity, we neglect the anisotropic screening effect. A periodic boundary condition has been used for the system in our calculation.

We know that in the discrete SSH model there are no analytic solutions; so the self-consistent numerical solution has to be determined. In this paper, we have used the simple iteration method. First, we define a bond variable $y(n)$ as

$$y(n) = u_{n+1} - u_n \quad (3)$$

and denote the electronic eigenstates by its wavefunctions $\phi_i(n)$ which diagonalizes the electronic part of the total Hamiltonian (equation (1)) and also satisfies the periodic boundary condition. Both $\phi_i(n)$ and $y(n)$ should be determined by the following coupled equations:

$$(\epsilon_i - V_n)\phi_i(n) = -[t_0 - \alpha y(n-1)]\phi_i(n-1) - [t_0 - \alpha y(n)]\phi_i(n+1) \quad (4)$$

$$y(n) = -\frac{4\alpha}{K} \sum_i' \phi_i(n)\phi_i(n+1) + \frac{4\alpha}{KN} \sum_n \sum_i' \phi_i(n)\phi_i(n+1) \quad (5)$$

where ϵ_i is the single-electron energy eigenvalue in the eigenstate $\phi_i(n)$, N is the total number of the lattice sites, and the prime on the summation in (5) means that the sum is restricted to the occupied single-electron eigenstates.

The coupled equations (4) and (5) can be solved by the following iteration procedure. First of all, we fix the positions of all N_{imp} impurity ions. As discussed above, the impurity ion distribution may be random or in an ordered phase; however, in this paper, we prefer to choose N_{imp} impurity ion sites in an almost ordered manner. Next we can calculate from equation (2) the Coulomb potential V_n produced by these ions. Then, choosing a set $\{y(n)\}$ of homogeneous values as their initial values and substituting them into (4), we can diagonalize it to find the eigenvalue ϵ_i and corresponding eigenfunctions $\{\phi_i(n)\}$. The $\phi_i(n)$ obtained are then substituted into equation (5) to obtain a new set of $\{y(n)\}$. The iteration is repeated until the difference between the new $\{y(n)\}$ and the old values becomes negligibly small.

In the calculation, the parameters are taken as follows: $K = 21 \text{ eV \AA}^{-2}$, $t_0 = 2.5 \text{ eV}$, $\alpha = 4.1 \text{ eV \AA}^{-1}$, $\epsilon = 10$, $a = 1.22 \text{ \AA}$ and $r_i = d = 2.0 \text{ \AA}$; the total number of lattice sites $N = 100$, and the total number of electrons $N_e = N + N_{imp}$. All the calculated results will be discussed in the following sections.

3. Band structure

For a chain of 100 sites and a set of numbers of impurity ions, $N_{imp} = 2, 4, 6, 8, 10, 12, 14, 16$, we have calculated the electronic energy bands, some of which are shown in table 1. It is easily seen that, when $N_{imp} = 12$, the gap between the soliton band edge and the valence band edge (hereafter called the lower gap) disappears; the gap between the soliton band and the conduction band (hereafter called the upper gap) almost disappears too, but it is still slightly larger than the average level spacing in the conduction band (about 7% larger). When $N_{imp} = 16$, no gaps exist. In order to see how the levels evolve with the impurity ion potential V_n we also calculate the bands for βV_n ($\beta = 0, 0.2, 0.4, 0.6, 0.8, 1.0$) and different doping concentrations. The results for $N_{imp} = 12$ are shown in figure 1. In contrast with the results obtained by Conwell *et al* [9], we find that the

potential V_n is not beneficial to gap closure but, on the contrary, increases the gap slightly around the Fermi surface. For example, when $\beta = 0$, i.e. without the ion potential, the values of both the upper and the lower gaps, are, in fact, less than the nearby level spacings in the conduction and valence bands for $N_{\text{imp}} = 12$. As β increases from zero, the largest effect of the potential is to make the whole bands move downwards. However, the upper gap becomes gradually slightly larger, but it has only a very small quantitative difference from the average level spacing around the Fermi surface until β is equal to 1. This is obvious from the fact that the essential effect on the gap closure comes from the average distance between two neighbouring soliton centres. When the distance becomes shorter than the soliton length, about 11 sites, the overlap between the electron wavefunctions in neighbouring soliton states is strong, which causes the gap to close. The exact value of impurity ion concentration $n_{\text{imp}} = N_{\text{imp}}/N$ at which the gap closure appears should not be considered seriously, and it is only consistent qualitatively with the experimental result because we neglect some important factors, e.g. interchain coupling, anisotropic screening and non-uniformity of doping existing in the real materials. The latter makes the impurity concentration in part of the doped sample larger than the average impurity concentration measured in experiments. Also, including the interchain hopping (three-dimensional effect) can much reduce the value of the gap calculated in one dimension. Experiments found the metal-insulator transition to occur at about $\langle n_{\text{imp}} \rangle \simeq 6-7\%$ for almost all the doped *trans*-polyacetylene irrespective of whether the impurity ion distribution is random or ordered. Therefore, we think that the randomness of the distribution has little effect on the gap closure and is not important even though it must have an effect on the electronic levels and wavefunctions. This is why we restricted our calculation to the ordered distribution of the impurity ions.

Table 1. Calculated electronic energy levels for a $(\text{CH})_x$ chain of 100 sites with different numbers N_{imp} of impurity ions.

$N_{\text{imp}} = 2$		$N_{\text{imp}} = 12$		$N_{\text{imp}} = 16$	
N	Energy level (eV/4.1)	N	Energy level (eV/4.1)	N	Energy level (eV/4.1)
45	-0.312 214	41	-0.646 799	39	-0.804 975
46	-0.253 978	42	-0.580 135	40	-0.742 239
47	-0.251 806	43	-0.578 364	41	-0.732 618
48	-0.204 580	44	-0.517 685	42	-0.662 888
49	-0.200 172		Lower gap		Lower gap
	Lower gap	45	-0.468 990	43	-0.644 017
50	-0.089 760	46	-0.419 792	44	-0.586 906
51	-0.088 830	47	-0.404 876	45	-0.570 019
	Upper gap	48-53	omitted	46-55	omitted
52	0.129 682	54	-0.121 638	56	-0.131 123
53	0.131 530	55	-0.119 162	57	-0.128 589
54	0.169 486	56	-0.073 702	58	-0.079 140
55	0.170 905		Upper gap		Upper gap
56	0.225 291	57	0.002 299	59	-0.019 661
		58	0.046 460	60	0.028 601
		59	0.050 802	61	0.031 264
		60	0.116 589	62	0.098 435

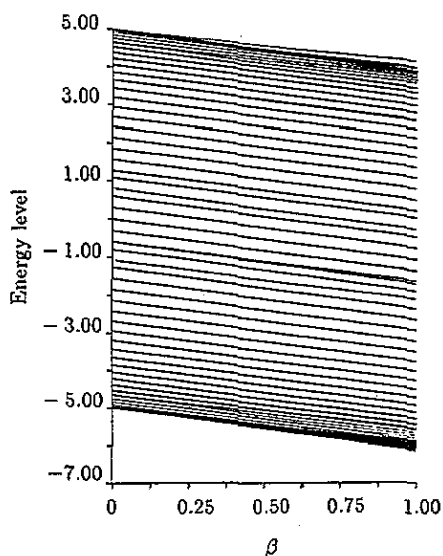


Figure 1. Calculated energy levels versus β (the fraction of the potential) for $N = 100$ (N is the number of sites) and $N_{\text{imp}} = 12$.

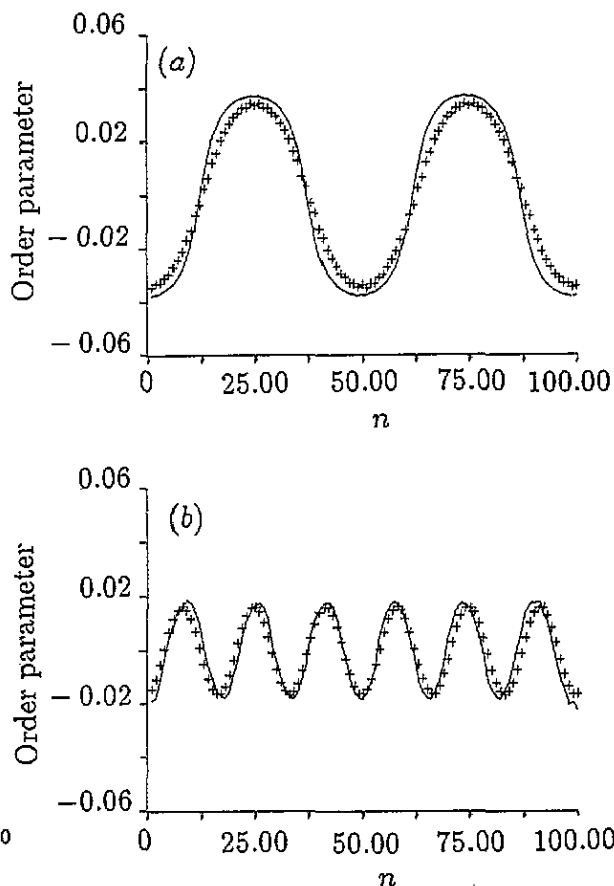


Figure 2. Calculated order parameter values Δ_s versus n for a chain of 100 sites for (a) $N_{\text{imp}} = 4$ and (b) $N_{\text{imp}} = 12$: +, $\beta = 0$; —, $\beta = 1$.

4. The order parameter of the soliton

In addition to electronic levels and wavefunctions we also calculate the order parameter Δ_s of solitons in order to see whether or not it becomes zero after the metal-insulator transition. The results for $N_{\text{imp}} = 4$ and 12 are shown in figure 2. For comparison, in these figures are also shown the results without the impurity ion potential ($\beta = 0$). We see from figure 2 that the potential has little effect on the order parameters. Two curves corresponding to the cases with the potential and without the potential, respectively, almost coincide with each other. This means that the periodic variation in the order parameter value is completely determined by the number of impurity ions N_{imp} . The total number of the maximum and minimum of the order parameter is equal to N_{imp} , and their positions are also determined by the positions of the impurity ions. The effect of the ion potential is only to make the maxima

slightly larger and the minima slightly smaller. On increase in the impurity concentration the potential effect becomes gradually smaller and smaller. Finally, after the gap disappears at $N_{\text{imp}} = 12$, the two curves for the order parameters with and without the potential totally coincide. On the other hand, the variation amplitude of the order parameter value becomes smaller and smaller too. However, more importantly, the decreasing rate of the amplitude is rather slow, e.g. the amplitude of Δ_s at $N_{\text{imp}} = 12$ is roughly half its value for the pure sample. Even though the band gap does not exist at all for the heavily doped sample, the order parameter is still not equal to zero. It seems that this phenomenon is similar to the superconductivity with no energy gap and consistent with the experimental observation of the infrared-active vibrational modes associated with solitons in heavily doped materials up to $y \simeq 18\%$.

5. Localization of the electronic wavefunctions

Knowing all the eigenstates from the self-consistent calculation, we can easily find the inverse participation ratio (IPR) of the eigenstate defined as

$$R_i = \sum_j |\phi_i(j)|^4 / \left(\sum_j |\phi_i(j)|^2 \right)^2. \quad (6)$$

Many researchers have used the IPR to estimate the degree of localization of eigenstates [15]. Figure 3 shows a distribution of our calculated IPR values on the eigenstates around the gap. For the low-doping case ($N_{\text{imp}} = 2$), two soliton states are localized in the gap. Adding the impurity potential to the system makes the two states more localized because their IPR values are twice those without the potential. Also those states lying on the upper edge of the valence band are more localized because of the effect of the potential. However, with increasing impurity concentration, the degree of localization for these states decreases rapidly so that, at $N_{\text{imp}} = 12$, there is no trace of the localization at all for the states. In contrast, when the impurity potential is introduced, their degree of localization is increased slightly. More probably, in this case we can no longer talk about localization of these wavefunctions; in fact, all these states are extended but have a small amplitude modulation which causes the charge density to be non-uniform along a chain and to have a periodic fluctuation along the chain because of the attractive impurity potential.

6. Summary

We have made a self-consistent numerical calculation based upon the SSH model plus the long-range Coulomb potential exerted by all impurity ions along a chain. The electronic band structure, the bond-alternation order parameter and the IPR values for all electronic eigenstates are calculated and discussed as functions of the doping concentration. The effect of the impurity potential on these quantities, especially on the band structures, are mainly considered in this paper. We found that, even though the potential does indeed have rather a large effect on the energy level distribution in the valence, conduction and soliton bands, it has only a small effect on the gap closure. Our results demonstrate that the larger overlap between the electronic wavefunctions in the nearest soliton states is the determining factor for gap closure, which is different from the result of Conwell *et al* [9]. They said that achievement of the metallic state requires both good wavefunction overlap in the soliton

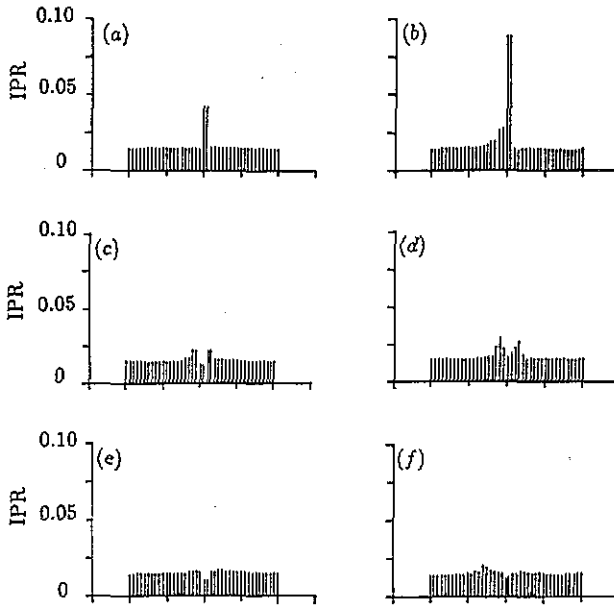


Figure 3. Distribution of the IPR (measured by the height of each vertical line) of the many eigenstates around the gap for the two cases of (a), (c), (e) $\beta = 0$ and (b), (d), (f) $\beta = 1$ with (a), (b) $N_{\text{imp}} = 2$, (c), (d) $N_{\text{imp}} = 6$ and (e), (f) $N_{\text{imp}} = 10$.

states and a deep potential well. The impurity potential is found to increase slightly the localization of the soliton states in the gap, the localization of the states at the top of the valence band and the localization of the states at the bottom of the conduction band. We also found that the order parameter Δ_s does not go to zero even in the heavy-doping region, and the impurity potential has only a small effect on the order parameter in the light-doping regime; with increase in the dopant concentration the effect becomes smaller and smaller, which is consistent with the experimental observations [11].

It is well known that there are two types of impurity: one is the site type [16], and the other is the bond type [17]. The former changes the site energy of π -electrons, but the latter changes the electron transfer energy. In this paper, we did not take into account the variation in the transfer integral due to doping at all. Therefore, our impurities belong to site-type category. As stated at the beginning we have not included the effect of the random distribution of the impurity ions for simplicity [18]. We think that the randomness might not be an important factor in the band closure at an impurity concentration of about 6–7% because many experiments indicate that the critical concentration is independent of the ion distribution (ordered or random). In addition, anisotropic screening is not considered, so that the dielectric constant ϵ takes the same value for different directions. Finally, our model is purely one dimensional, and the three-dimensional effect has been completely omitted in our calculation. Including the three-dimensional effect might reduce the value of the critical concentration at which the gap closure appears.

References

- [1] Heeger A J, Kivelson S A, Schrieffer J R and Su W P 1988 *Rev. Mod. Phys.* **60** 781

- [2] Naarmann H 1987 *Synth. Met.* **17** 2223
- [3] Su W P, Schrieffer J R and Heeger A J 1979 *Phys. Rev. Lett.* **42** 1698; 1980 *Phys. Rev. B* **22** 2099
- [4] Epstein A J, Bigelow R W, Rommelmann H, Gibson H W, Weagley R J, Feldblum A, Tanner D B, Pouget J P, Pouxviel J C, Comes R, Robin P and Kivelson S 1985 *Mol. Cryst. Liq. Cryst.* **117** 147
- [5] Dong J 1984 *PhD Thesis* University of California at Santa Barbara
- [6] Kivelson S and Heeger A J 1985 *Phys. Rev. Lett.* **55** 308
- [7] Sheng P 1980 *Phys. Rev. B* **21** 2180
- [8] Mele E J and Rice M J 1981 *Phys. Rev. B* **23** 5397
- [9] Conwell E M, Mizes H A and Jeyadev S 1989 *Phys. Rev. B* **40** 1630; 1990 *Phys. Rev. B* **41** 5067
- [10] Chen J and Heeger A J 1988 *Synth. Met.* **24** 311
- [11] Tanner D, Doll G, Rao K, Yang M H, Eklund C, Arbuckle G and MacDiarmid A G 1987 *Bull. Am. Phys. Soc.* **32** 422
- [12] Conwell E M and Jeyadev S 1987 *Phys. Rev. Lett.* **61** 361
- [13] Bryant G W and Glick A J 1982 *Phys. Rev. B* **26** 5855
- [14] Bulka B R 1988 *Synth. Met.* **24** 41
- [15] Stafstrom S and Chao K A 1984 *Phys. Rev. B* **30** 2098
- [16] Harigaya K, Wada Y and Fesser K 1990 *Phys. Rev. B* **42** 1276, 11 303
- [17] Harigaya K, Wada Y and Fesser K 1990 *Phys. Rev. B* **42** 1268
- [18] Harigaya K, Terai A and Wada Y 1991 *Phys. Rev. B* **43** 4141